

EFFECTS OF TRANSIENT CSR WAKEFIELDS ON MICROBUNCHING IN A BUNCH COMPRESSOR*

C. Mitchell and J. Qiang, LBNL, Berkeley, CA 94720, USA

Abstract

The standard analytical treatment of CSR-induced microbunching in a bunch compressor chicane makes use of a steady-state 1-D model of the longitudinal CSR interaction. This model is numerically generalized to include the effect of transient CSR wakefields due to bend entry and exit, as well as CSR that is generated in upstream bends and propagates across one or more lattice elements before interacting with the beam. The resulting linear integral equation for CSR-induced microbunching is solved numerically for the second bunch compressor of a proposed Next Generation Light Source.

INTRODUCTION AND MOTIVATION

In high-brightness light sources such as X-ray free-electron lasers (FELs), the presence of collective effects such as coherent synchrotron radiation (CSR) can result in a microbunching instability in which large-amplitude current modulations grow from small amplitude modulations present in the initial current profile, thereby decreasing the beam quality into the FEL. The CSR-induced microbunching is of particular concern in bunch compressor chicanes, and the growth of this instability has been well-studied using a 1-D ultrarelativistic model of the CSR interaction [1, 2]. This model assumes a steady-state form of the CSR in the bending dipoles that is valid at distances greater than $(24\sigma R^2)^{1/3}$ from the bend entry, where σ is the rms bunch length and R is the bending radius. In addition, bend exit radiation that follows the beam into a succeeding drift is neglected.

Extended 1-D models of the longitudinal CSR interaction are available that are valid over a larger range of energies, and that include the transient effects resulting from bend-drift transitions [3]. Recent models also include the effects of radiation emitted within upstream bends that follows the bunch downstream through multiple lattice elements before interacting with the beam [4]. The linear theory of the microbunching instability can be extended using these improved models to check the regime of validity of a steady-state treatment.

A MICROBUNCHING EQUATION SOLVER

The growth of the CSR-induced microbunching instability in a chicane at an uncompressed wavelength $\lambda_0 =$

$2\pi/k_0$ is described by the linear integral equation [1, 2]:

$$b[k(s), s] = b_0[k(s), s] + \int_0^s d\tau K(s, \tau) b[k(\tau), \tau], \quad (1)$$

where $k(s) = k_0 C(s)$ is the compressed wavenumber, C is the compression factor, and the bunching factor b is given in terms of the beam distribution function f by:

$$b(k, s) = \frac{1}{N} \int e^{-ikz} f(\vec{X}) d\vec{X}. \quad (2)$$

The kernel $K(s, \tau)$ is determined by the beam and lattice parameters and the impedance of the CSR interaction, which we write in the form:

$$Z(k, s) = \int_0^\infty e^{-ik\zeta} K_{CSR}(\zeta, s) d\zeta, \quad (3)$$

where $K_{CSR} = q\vec{n} \cdot \vec{E}$ is the kernel for the longitudinal CSR interaction provided in [4], given as a function of the separation ζ between source and observation points within the beam.

The integral equation (1) is solved using a numerical marching method in the coordinate s , which measures the path length along a design trajectory through the lattice. The design trajectory is assumed to consist of a set of straight-line segments (in the drifts) and circular arcs (in the bends). At each lattice step, the Fourier integral (3) is evaluated using an integrated Green function method together with an FFT [5], and we choose a Nyquist wavelength much shorter than the smallest wavelength of interest to avoid aliasing effects. The quadrature in (1) is then evaluated by a trapezoidal rule using the results for b obtained at previous steps.

Two primary input parameters are the integers **nel - drifts** and **nel - bends** that denote the number of beamline elements to be included in the CSR computation when the bunch centroid lies within a drift and a bend, respectively. Table 1 indicates how various assignments of these parameters are related to the 1-D CSR models described in [3, 4]. Particles whose computed retarded position lies outside the lattice do not contribute to the CSR computation.

Benchmark

As a numerical benchmark, we examine the microbunching gain in the chicane of the 2nd LCLS bunch compressor using parameters provided in [1, 2]. The result obtained using the steady-state CSR model (**nel** = 1) is shown in Fig. 1. This is to be compared with a similar result reported in [1] that was obtained by numerically solving the integral equation (1) using an analytical form of the ultrarelativistic steady-state CSR impedance.

* Work supported by the U.S. Department of Energy under Contract No. DE-AC02-05CH11231.

Table 1: Solver input parameters for comparing CSR effects in a 4-bend magnetic chicane.

CSR model	nel - drifts	nel - bends
Steady-state	1	1
Cases A & B [3] (entry transients)	1	2
Cases B-D [3] (exit transients)	3	1
Cases A-D [3]	3	2
Nearest upstream bends [4]	3	4
Full chicane lattice [4]	6	7

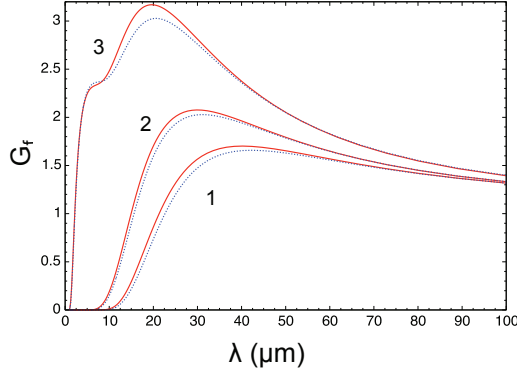


Figure 1: Microbunching gain for the second LCLS bunch compressor computed using the parameters in [2] in the presence of steady-state CSR. The result is shown as a function of uncompressed wavelength. Dashed lines denote numerically computed results, while solid lines are obtained using the approximate analytical expressions in [2]. A similar calculation is reported in [1].

FIELD ENHANCEMENT AND IMPEDANCE

As motivation for studying transient microbunching effects, consider an electron bunch of rms length σ_z with a gaussian longitudinal profile propagating into a bend. We assume that the bunch possesses a density modulation at a wavelength $\lambda_m \ll \sigma_z$, which we write as

$$\lambda(z) = \bar{\lambda}(z)(1 + \mathcal{R}e(Ae^{ik_m z})) \quad (4)$$

where A is the complex amplitude of the modulation, $k_m = 2\pi/\lambda_m$, and $\bar{\lambda}$ is the unperturbed gaussian density.

Fig. 2 illustrates the longitudinal CSR wakefield generated by a 300 pC gaussian bunch with the parameters $\sigma_z = 287 \mu\text{m}$, $\lambda_m = 6 \mu\text{m}$, and $A = 3\%$ at 721 MeV. The bend is assumed to have a radius of $R = 2.78 \text{ m}$. (See Table 2.) The energy loss per unit length along the bunch is shown at a distance of 5 cm into the bend, scaled by the value $W_0 = 72 \text{ keV/m}$. The red curve denotes the wakefield obtained using the density (4), while the blue curve denotes the wakefield obtained using the unperturbed density $\bar{\lambda}$. The result is computed using the 1-D model of [3], which includes bend entry transient effects. Note that the wakefield is strongly enhanced at a wavelength of $6 \mu\text{m}$,

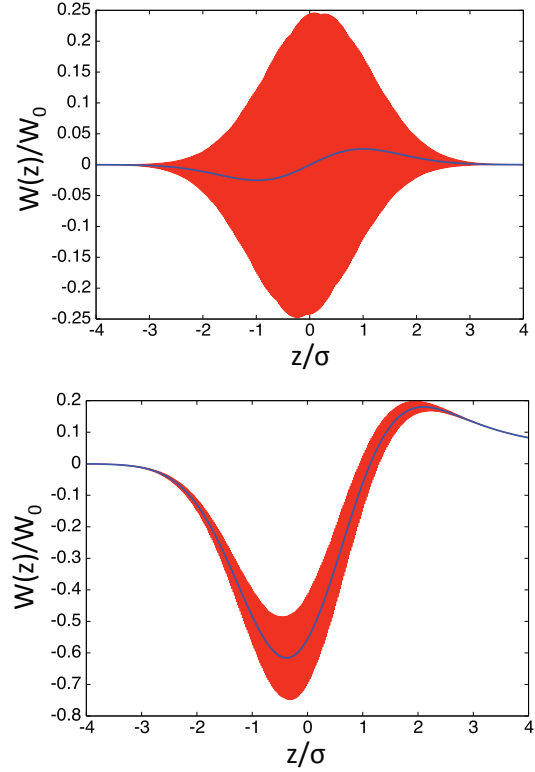


Figure 2: The wakefield generated by a gaussian bunch with a 3% density modulation. (Upper) The wakefield at 5 cm into the bend when entry transient effects [3] are included. (Lower) The wakefield obtained using a steady-state model of CSR. The amplitude of the modulation can be predicted using (5).

and the relative amplitude of this modulation is a factor of 40 larger than is predicted by the steady-state model.

Using the ultrarelativistic model for the wakefield in a bend described in [6], the transient CSR impedance can be evaluated analytically to give:

$$\frac{Z(k)R\phi}{r_c m c^2} = -4 \left[e^{-i\mu} - e^{-4i\mu} + (i\mu)^{1/3} f(\mu) \right], \quad (5)$$

where

$$f(\mu) = \Gamma\left(\frac{2}{3}\right) - \Gamma\left(\frac{2}{3}, i\mu\right), \quad (6)$$

ϕ is the entry angle of the bunch centroid into the bend, and $\mu = kR\phi^3/24$ is a dimensionless parameter characterizing the wavenumber. Fig. 3 illustrates the quantity (5), which is shown together with the corresponding steady-state result. As a consequence of variations appearing in the impedance, the transient wakefield at some wavenumbers is enhanced relative to the steady-state result, while at others it is suppressed. The density modulation at $6 \mu\text{m}$ is enhanced by the peak appearing in the real part of the impedance at $\mu = 0.7$. In the following section, we investigate the net effect, if any, such field enhancement has on the microbunching gain in a realistic magnetic chicane.

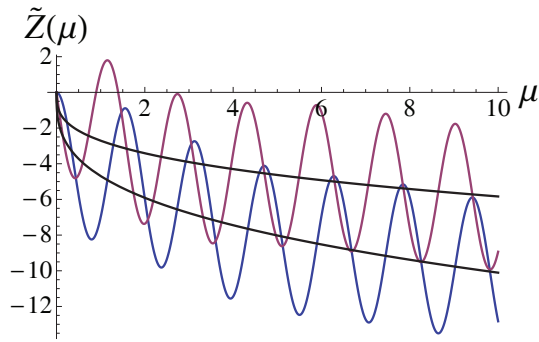


Figure 3: The ultrarelativistic transient CSR impedance in a bend (5) is shown together with the steady-state limit. The real part appears in blue, while the imaginary part appears in red. Enhancement of the real part of the impedance at $\mu = 0.7$ is clearly visible.

NEXT GENERATION LIGHT SOURCE

The algorithm described here was used to investigate the CSR-induced microbunching gain in the second bunch compressor of a proposed Next Generation Light Source X-ray FEL being studied at Lawrence Berkeley National Laboratory [7]. Basic parameters for the chicane are provided in Table 1. We assume no laser heating, so that the beam has an uncorrelated energy spread at the chicane entry of about 4 keV.

Table 2: Parameters for NGLS BC2 gain calculation.

Chicane parameters	symbol	value
Bend magnet length	L_B	0.25 m
Drift length (B1→B2, B3→B4)	ΔL	4.5 m
Drift length (B2→B3)	L_c	2.64 m
Bend angle	$ \theta $	5.16 deg
Bend radius	$ R $	2.78 m
Momentum compaction factor	R_{56}	-75.0 mm
Electron beam parameters	symbol	value
Nominal energy	E_0	721 MeV
Initial peak current	I_0	100 A
Uncorr. initial rms energy spread	$\sigma_{\delta 0}$	5.5×10^{-6}
Linear energy chirp	h	10.6 m^{-1}
Initial rms bunch length	σ_{z0}	287 μm
Final rms bunch length	σ_{zf}	57.4 μm
Initial rms norm. emittance	$\gamma\epsilon_x$	0.7 μm
Initial beta functions	β_{x0}	58.77 m
Initial alpha functions	α_{x0}	3.09

The resulting gain is illustrated in Fig. 4 for three of the parameter settings shown in Table 1. The steady-state result is comparable to the LCLS result of Fig. 1. Modeling transient wakefield effects in the bends due to bend entry effects reduces the gain by $\sim 5\%$. Modeling transient wakefield effects in the drifts due to bend exit effects increases the gain by $\sim 17\%$, and modeling the effect of upstream radiation from the the preceding bends has negli-

gible effect on the gain at these parameters. Notice that the

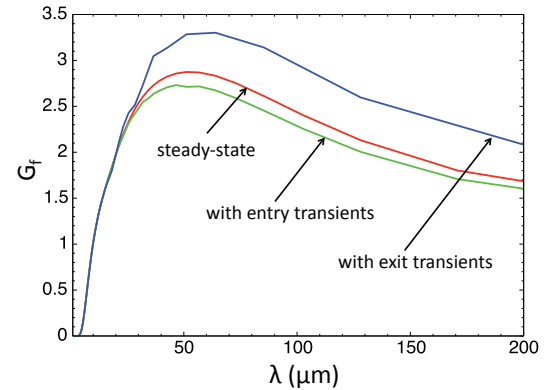


Figure 4: The microbunching gain for the second NGLS bunch compressor is shown as computed using several models of CSR. The gain obtained with upstream bend effects included is indistinguishable from the blue curve shown here. All results are shown as functions of the uncompressed wavelength.

large field enhancement visible at a wavelength of 6 μm (Fig. 2) has little effect on the final microbunching gain. The longitudinal slippage induced by the initial beam energy spread and transverse beam size effectively suppresses modulations with wavelengths less than 20 μm . Even when the slippage is negligible, variations in the bend transient impedance that result in field enhancement (corresponding to the peaks in Fig. 3) are averaged away as the bunch propagates through the bend.

Additional parameter studies are required to investigate the dependence of the transient gain on the initial beam parameters and the chicane R_{56} .

ACKNOWLEDGMENT

This research used computer resources at the National Energy Research Scientific Computing Center and at the National Center for Computational Sciences.

REFERENCES

- [1] S. Heifets and G. Stupakov, Phys. Rev. ST Accel. Beams 5 (2002) 064401.
- [2] Z. Huang and K.J. Kim, Phys. Rev. ST Accel. Beams 5 (2002) 074401.
- [3] E.L. Saldin, E.A. Schneidmiller, and M.V. Yurkov, Nucl. Instrum. and Meth. in Phys. Res. A 398 (1997) 373-394.
- [4] D. Sagan, G. Hoeffstaetter, C. Mayes, and U. Sae-Ueng, Phys. Rev. ST Accel. Beams 12 (2009) 040703.
- [5] C. Mitchell, J. Qiang, and R. Ryne, Nucl. Instrum. and Meth. in Phys. Res. A 715 (2013) 119-125.
- [6] G. Stupakov and P. Emma, Proc. of EPAC 2002, Paris, France (2002) 1479-1481.
- [7] J. Corlett et al, Proc. of ICAP 2012, New Orleans, LA (2012) 1762-1764.